Performance of different classes of Filtering Facepiece Respirators toward nanoparticles

C. Brochot[1*] and A. Bahloul[1]

[1] Research Department, Institut de recherche Robert-Sauvé en santé et en sécurité du travail, Montréal, Canada.

* Corresponding author E-mail: Clothilde.brochot@irsst.qc.ca

ABSTRACT

Introduction: In the case of exposure to harmful substances and the use of a filtering facepiece respirator (FFR) to protect workers, it is important to know the performance of commercial FFR. In previous studies, the authors investigated a series of parameters on the effectiveness of a standard N95 FFR: particle diameter, airflow rate intensity, breathing simulation, time of use, relative humidity. It remains uncertain whether previous results can be extrapolated to all commercial FFRs.
Objective: To determine whether previous conclusions apply to other FFRs, an expanded selection of models was evaluated in this study. The initial penetrations are then measured in order to compare the penetrations amongst the different FFRs.
Methods: To do so, an experimental setup generates NaCl nanoparticles before introducing them into a test chamber containing the FFR. A constant flow of 85 L/min is drawn through the FFR and particle concentration is measured upstream and downstream of the FFR with a Scanning Mobility Particle Sizer. This setup allows penetration to be measured as a function of the particle diameter from 10 to 200 nm. Pressure drop was also measured across the FFR.
Results: The benchmark established in this study confirms that penetration measurements align with previously reported values. All tested FFRs exhibit comparable trends: the most penetrating particle size (MPPS) remains between 30 and 50 nanometers, with penetration decreasing for particles smaller or larger than this range.
Conclusion: The results obtained thus indicate that the outcome achieved previously for the standard N95 FFRs can be extrapolated to the other FFRs presented here.

Keywords: Filtering facepiece respirators, electret, NaCl, classification, efficiency, penetration.

INTRODUCTION

In some workplaces, there are numerous exposures to chemical, biological, particulate and other substances, or mixtures. These exposures are due to the use of chemicals, hazardous substances and industrial processes, such as the use of tools or the implementation of particular tasks, all in a generally closed or semi-closed environment. Nano-sized particles are generated by manufacturing processes such as welding, combustion, vapor deposition, or gaseous phase synthesis. These particles are commonly found in the indoor air of many workplaces (NIOSH, 2021; Andraos *et al.*, 2022). Employers have become aware of the toxicity of these particles, whose diameter is less than 100 nanometers. Indeed, studies have shown that these nano-sized particles, because of their large specific surface area, exhibit greater biological activity for the same mass, making them more toxic than larger particles of the same chemical composition (Schraufnagel, 2020; Chen *et al.*, 2023). Moreover, as nanotechnologies are becoming more and more common in many work environments (automotive, aerospace, transportation, etc.), worker's exposure to these nano-sized materials is growing (NIOSH, 2021; Andraos *et al.,* 2022).

In the case of these types of exposures, employers must implement solutions to protect the health of its workers with various means of control; hierarchically ranked according to their effectiveness (NIOSH 2015). Respiratory protective devices, such as FFRs are therefore a last measure to protect workers from

substances harmful to health when they are performing their work. It is thus legitimate to question their performance (filtration efficiency) against nano-sized particles. Among all commercially available FFRs, the N95 FFR is probably the most widely used device. The N95 FFR achieves high filtration efficiency – typically above 95% - through electrostatic attraction within its charged filter layers, which effectively captures nano-sized particles (Abdolghader *et al.*, 2018; Essa *et al.*, 2021; O'Shaughnessy *et al.*, 2022).

Indeed, currently and in North America, FFRs are classified according to 42 Code of Federal Regulations, part 84 (Code of Federal Regulations 1995) and CSA Z94.4.1:21 (CSA 2021). These standards classify FFRs according to the exposure aerosol (N, R and P), the minimum total efficiency of the FFR (95, 99 and 100) and, in the case of the Canadian standard, the initial pressure drop (3.43 mbar, 1.75 mbar and 1.00 mbar). With these standards, FFR are tested using charge-neutralized NaCl aerosol (for FFR classified N) and DOP aerosol (for FFR classified R or P), with an 85 liters per minute (Lpm) constant flow and up to 200 mg challenge aerosol load. For NaCl aerosol, the count median diameter (CMD) is approximately 75 nanometers, and the geometric standard deviation (GSD) is 1.86. For DOP aerosol the CMD is approximately 185 nanometers, and the GSD is 1.60. Concentration measurements upstream and downstream of the FFR are collected with a photometer or equivalent instrumentation, and the ratio of aerosol concentrations gives the penetration value. The certification criterion for N95 FFR is as follows: the total particle penetration limit is 5% (calculated in mass). The NIOSH certification test is generally tested using a TSI 8130 Automated Filter Tester. This device uses a forward light scattering photometer to measure the particle concentrations. One can note that the photometer is not capable of adequately measuring light scatter of particles below approximately 100 nanometers in diameter (Eninger *et al.* 2008), reducing the contribution of nanoscale particles to the penetration measurement. Also, certified total penetration is calculated, in mass, and does not provide information on efficiency as a function of particle diameter. Furthermore, in the case of electret media, the most penetrating particle size (MPPS) is typically less than 100 nm. In order to provide users with real performance data based on the particles they are exposed to, the most practical solution is to measure penetration as a function of particle diameter over a diameter range that includes the MPPS, i.e. between 10 and 200 nm (Rengasamy *et al.* 2011; Corbin *et al.* 2021).

Before the COVID-19 pandemic, some studies compared the laboratory performance of different FFRs (typically comparisons were between different FFRs or during fit factor measurements). But during the pandemic, studies with a benchmark approach have been published to compare the penetration of different FFRs as a function of particle size, or to compare surgical masks or homemade masks with FFRs as a function of particle size FFRs (Hao *et al.* 2020; Konda *et al.* 2020; Brochot *et al.* 2020a, 2020b; O'Shaughnessy *et al.* 2021; Zangmeister *et al.* 2020; Bourrous *et al.* 2021; Drewnick *et al.* 2021; Sharma *et al.* 2022). Since the end of the pandemic, some researchers have continued to work on respiratory protective devices, and more precisely on FFRs, but with a focus on fit (McAvoy *et al.* 2021; Ng *et al.* 2022; Freeman *et al.* 2022; Marchais *et al.* 2025), on FFR as a source-control device (Asadi *et al.* 2020; Bahloul *et al.* 2021; Yang *et al.* 2025a and 2025b) or on a hospital environment use, and especially with regard to decontamination (Peters *et al.* 2021; Kumar *et al.* 2022; Sharma *et al.* 2022; Zhu *et al.* 2022; Turgeon *et al.* 2023; Kim *et al.* 2024).

In the previous work, IRSST's working group (Institut de recherche Robert-Sauvé en santé et en sécurité du travail; the occupational health and safety research institute in Quebec, Canada) has already studied in detail the penetration of one specific N95 FFR. The authors have studied the effect of the airflow rate, the constant or cyclic breathing pattern, the time of use and the relative humidity (Bahloul *et al.* 2014; Mahdavi *et al.* 2014, 2015; Brochot *et al.* 2015, 2020a). These studies led to the development of a reliable method for measuring FFR penetration and highlighted the following trends: The MPPS for the tested N95 FFRs was approximately 50 nanometers, and the filtration efficiency exceeded 95% at 85 L/min, as required by certification. However, at higher flow rates—135, 270, and 360 L/min—the filtration efficiency dropped below the 95% threshold, reaching about 85%. A constant flow rate equal to the average breathing flow rate (Vmin) underestimates penetration compared to cyclic flow mode, while using a flow rate equivalent to the maximum cyclic flow rate (peak inspiratory flowrate, PIF) overestimates the particle penetration. The constant flow rate equivalent to the mean inhalation flow rate (MIF), i.e. 2 x Vmin, provides a better

prediction of the penetration of the N95 FFR in cyclic flow mode. The MPPS shifts toward larger particle sizes as clogging increases, due to the loss of electrostatic charge in the electret media. At 10% relative humidity, penetration decreases over time, whereas at 80% relative humidity, penetration increases.

Nevertheless, the question remained whether these observations can be applied to other FFRs. In this study, the authors first compared the initial penetrations of different FFRs under conditions provided by our established setup and checked whether certain parameters could limit this comparison and interpolation. A wide variety of additional FFRs were selected from different manufacturers representing diverse characteristics: with or without exhalation valve, with different filtering surfaces, and with different classifications. The penetration of NaCl nanoparticles was measured in order to assess the penetration values for particles between 10 to 200 nm. Pressure drop was also measured for each selected FFR.

METHODS

Selected Filtering facepiece respirators (FFRs)

Twelve different commercially available FFRs were selected for this study. Table I shows the different characteristics of the FFRs, such as their class according to 42 CFR 84, their shape, their origin, and geometric surface area. All twelve FFRs contain an electret medium enclosed by other inner and outer layers in order to soften the device, protect the medium or limit the moisture inside. Also, some surface areas were evaluated and presented in Table I.

The FFR samples were randomly selected from the different boxes of FFRs stored in our laboratory and tested without conditioning.

The first FFR is the specific N95 FFR studied previously. The first six FFRs are entry-level FFRs from three different manufacturers, with N95 classification, and with and without valve. FFR_A1, FFR_A1v, FFR_A2, FFR_A2, FFR_A3, FFR_A4v, FFR_A5, FFR_A6v and FFR_A7v are from the same manufacturer and have specificities: FFR_A2 has a larger filter surface area; FFR_A3 is designed to improve the fit; FFR_A4v is conceived for a welding fume exposition; FFR_A5 is certified R95; FFR_6v is certified P95; and FFR_A7v is certified N100.

Experimental filtration performance setup

The test setup used in this study is the same presented in our previous studies (Bahloul *et al.* 2014; Mahdavi *et al.* 2014, 2015; Brochot *et al.* 2015, 2020b, 2020c, 2021). This setup was used to measure the pressure drop Δp (mbar) and the filtration efficiency E (%) of a FFR, with a 85 L/min constant airflow rate).

The setup is composed of a Collison nebulizer with 6 jets (CN 2425, CH Technologies, USA) which generate NaCl nanoparticles (NaCl concentration at 0.1% v/v). The particles are dried with a diffusion drier and brought to Boltzmann equilibrium with an 85Kr radioactive source (TSI model 3054A from TSI Inc., Shoreview, MN, USA). The polydispersed aerosol thus generated comprises particles ranging from 10 to 400 nm and centered at around 70 nm, based on the electrical mobility diameter.

Table I. Filtering Facepiece Respirators (FFRs) used in this study.

Designation	Manufac-turer	Classification according to 42 CFR 84	Surface area ($cm^2 \pm 5cm^2$)	External description
FFR_A1	Manuf. A	N 95	190	Cup shape without valve
FFR_A1v	Manuf. A	N 95	170	Cup shape with valve
FFR_B	Manuf. B	N 95	--	Cup shape without valve
FFR_Bv	Manuf. B	N 95	--	Cup shape with valve
FFR_C	Manuf. C	N 95	210	Cup shape without valve
FFR_Cv	Manuf. C	N 95	200	Cup shape with valve
FFR_A2	Manuf. A	N 95	320	Flat folded without valve
FFR_A3	Manuf. A	N 95	220	Flat folded without valve
FFR_A4v	Manuf. A	N 95	170	Cup shape with valve
FFR_A5	Manuf. A	R 95	190	Cup shape without valve
FFR_A6v	Manuf. A	P 95	170	Cup shape with valve
FFR_A7v	Manuf. A	N 100	--	Cup shape with valve

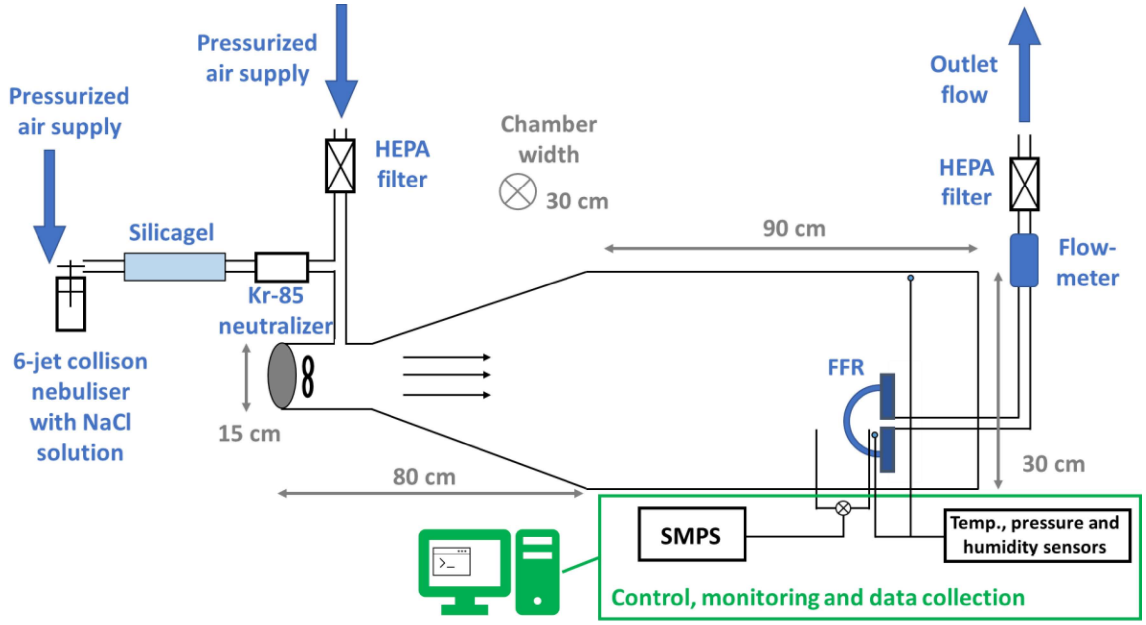


Figure 1. Experimental test bench used to measure the filtering facepiece respirators.

The aerosol is then injected into the test chamber in which the FFR is installed. The FFR is sealed onto a

plate using a metal template and four fixings. The plate is coupled to a pump and set at a constant airflow rate of 85 Lpm, as recommended by 42 CFR 84 to simulate constant inhalation flow. Aerosol concentrations were then collected upstream and downstream of the FFR and directed to the Scanning Mobility Particle Sizer, SMPS (TSI Model 3080, 3081, 3775 From TSI Inc., USA) coupled with an advanced aerosol neutralizer (TSI Model 3087 From TSI Inc., USA) with measured particle size distributions across 21 channels covering a range from 10 to 200 nanometers. Three particle size distributions are collected upstream of the FFR, followed by three distributions downstream and two distributions upstream in order to verify the stability of the generation throughout the measurement. The first three concentration samples upstream and three concentration samples downstream are used to calculate the average penetration of the tested FFR, at each of the 21 channels measured by the SMPS according to Equation 1. The penetration results presented in this paper are the means and standard deviations for three samples of FFRs tested (N = 3).

$$E = 1 - P = 1 - \frac{C_{downstream}}{C_{upstream}} \quad (1)$$

The pressure drop is measured according to equation 2, using a FLUKE 922 differential pressure sensor (Fluke corp., Everett, WA, USA). This instrument has a measuring range of ± 40 mbar, with a reading accuracy of ± 1%, i.e. 0.4 mbar.

$$\Delta p = p_{upstream} - p_{downstream} \quad (2)$$

RESULTS

Comparison of initial penetration results – Effect of valve and manufacturer

Figure 2 presents penetration measurements for the first six FFRs listed in Table I. These entry-level N95 respirators, from three manufacturers, include models with and without exhalation valves. Penetration is shown as a function of electrical mobility particle diameter, ranging from 10 to 200 nanometers.

All six of these entry-level FFRs exhibited maximum penetration values below the normative limit of 5%. The MPPS was between 40 - 50 nanometers, and the presence of a valve does not affect MPPS. However, penetration increases slightly when a valve is present. For example, FFR_A1 and FFR_A1v show maximum penetrations of (2.84 ± 0.95)% and (3.85 ± 0.86)% respectively; FFR_B and FFR_Bv show (2.52 ± 0.35)% and (3.25 ± 0.09)%; and FFR_C and FFR_Cv show (2.67 ± 0.63)% and (3.13 ± 2.06)%. This increase may be explained by the valve reducing the filtration area by approximately 10–20 cm², which raises filtration velocity.

Overall, the valve slightly increases maximum penetration but does not alter penetration trends by particle size: MPPS remains unchanged, and penetration decreases similarly for particles smaller or larger than MPPS.

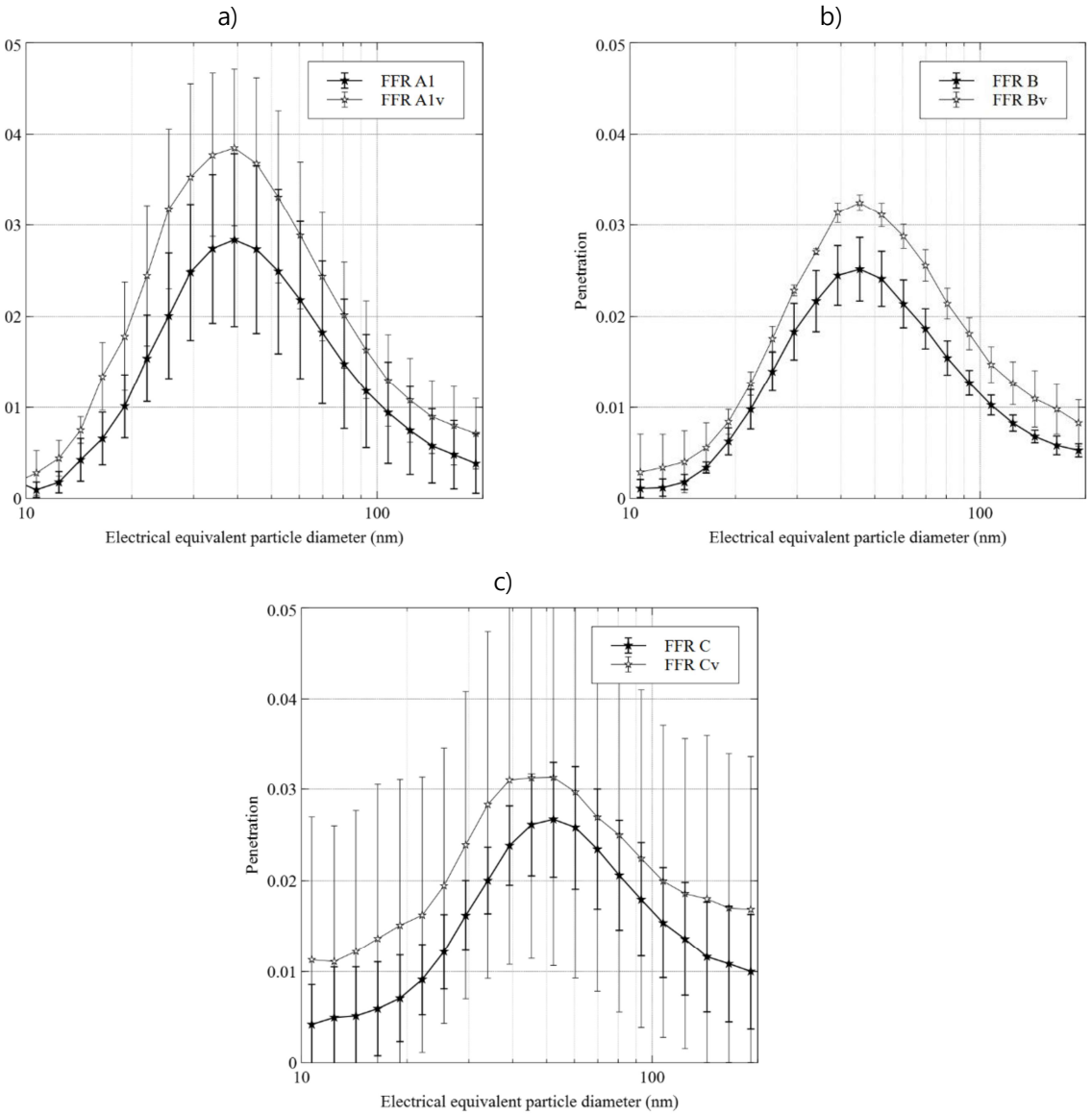


Figure 2. Mean penetrations (N = 3) ± standard deviation for a) FFR_A1 and FFR_A1v, b) FFR_B and FFR_Bv and c) FFR_C and FFR_Cv.

Comparison of penetration results at initial - N95 FFRs with different parameters

Figure 3 shows penetration measurements for FFR_A2, FFR_A3, and FFR_A4v, all produced by Manufacturer A. Gray shading represents the standard deviation of penetration for FFR_A1, included for comparison. FFR_A1 is the entry-level N95 model, while the other three have enhanced design features: FFR_A2 offers a very large filtering area to ease breathing; FFR_A3 combines a large surface with improved fit; and FFR_A4v is intended for welding fumes, incorporating additional seals for fit and a charcoal layer to reduce organic vapor concentrations.

The maximum penetration values for these three FFRs are below the normative limit of 5% and lower than those observed for FFR_A1. Their MPPS consistently are between 30 - 50 nanometers. These results indicate that design variations—such as larger filter areas or added features for specific applications—reduce maximum penetration without altering penetration trends by particle size. MPPS remains stable or slightly lower, and penetration decreases similarly for particles smaller or larger than MPPS.

Comparison of initial penetration results - Effect of classification

Figure 4 shows penetration measurements for FFR_A5, FFR_A6v, and FFR_A7v, all produced by Manufacturer A. Gray shading represents the standard deviation of penetration for FFR_A, the entry-level N95 model, included for comparison. The three respirators tested are classified as R95, P95, and N100, respectively. N-rated FFRs are intended for oil-free aerosols, while R- and P-rated models are suitable for environments containing oil-based particles—R for short-term use and P for extended use.

The maximum penetration values for these FFRs are well below the normative limit of 5% and significantly lower than those observed for FFR_A1. Their MPPS are between 30 - 40 nanometers. For FFR_A7v, classified as N100, the minimum efficiency measured was 99.98 ± 0.01%, exceeding the normative requirement of 99.97%. These results indicate that higher-efficiency ratings substantially reduce penetration without altering penetration trends by particle size. MPPS remains stable, and penetration decreases similarly for particles smaller or larger than MPPS.

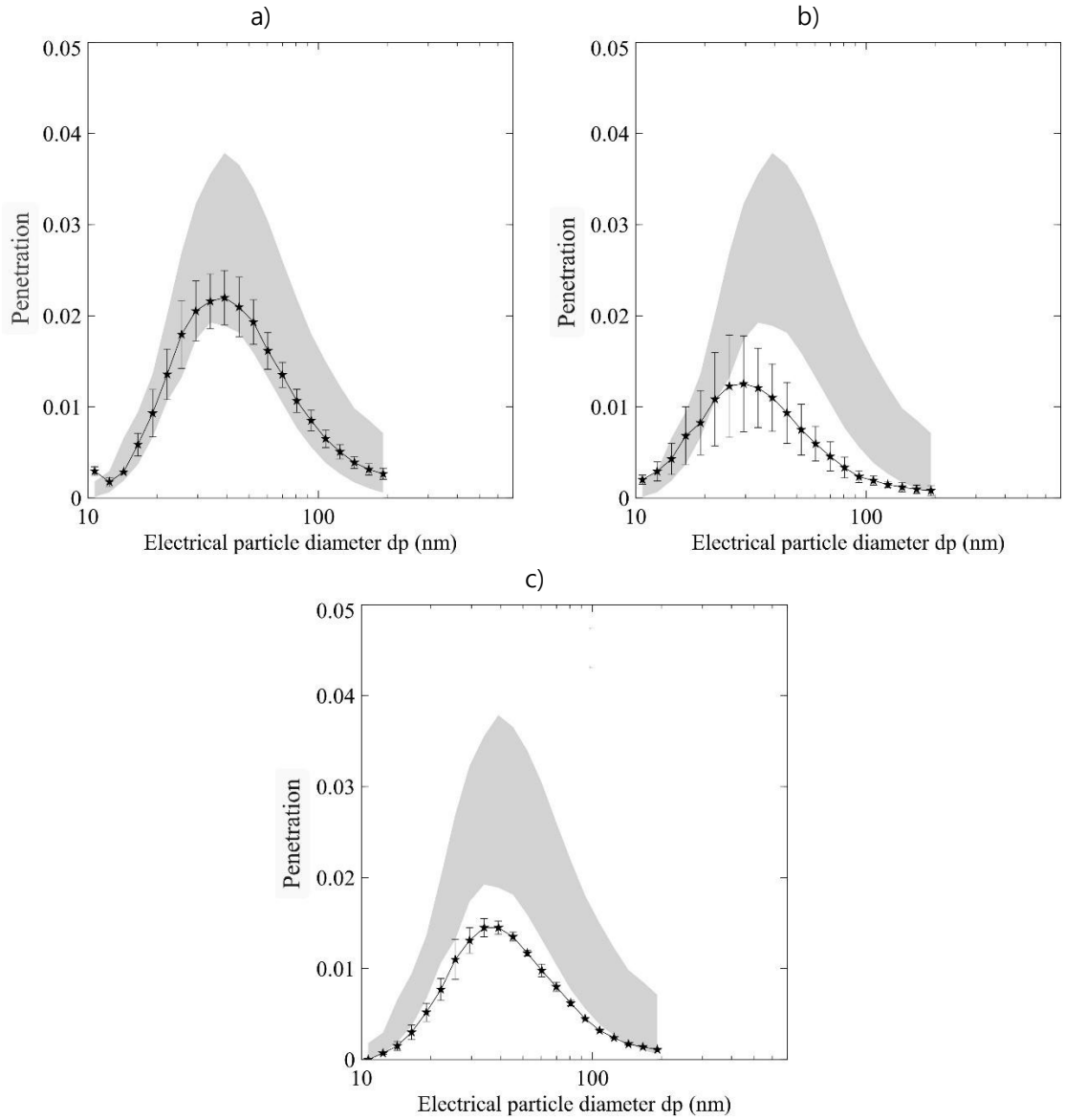


Figure 3. Mean penetrations (N = 3) ± standard deviation for a) FFR_A2, b) FFR_A3 and c) FFR_A4v (the grey area represents the average penetration (standard deviation) of FFR_A1, as reference).

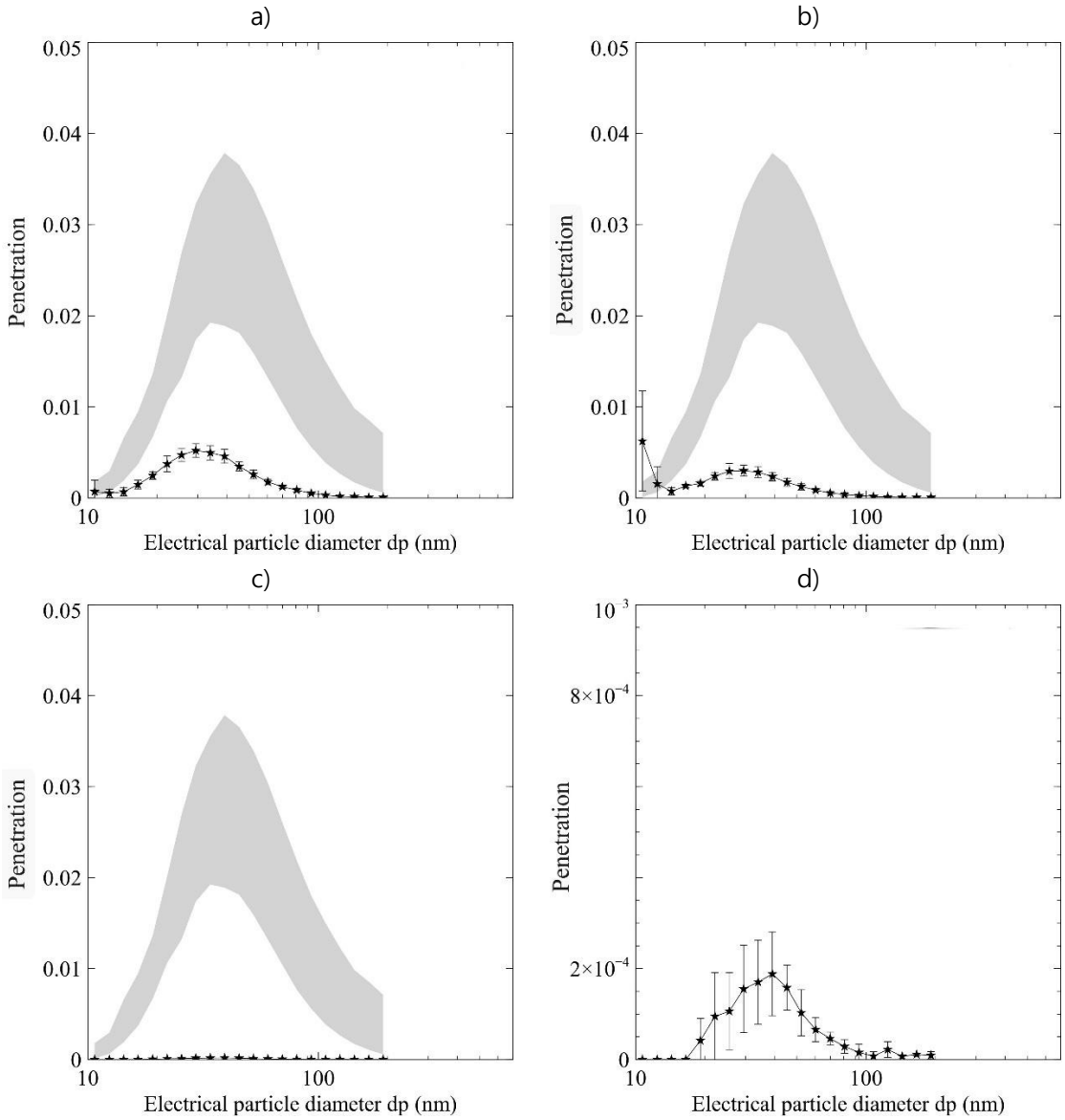


Figure 4. Mean penetrations (N = 3) ± standard deviation for a) FFR_A5, b) FFR_A6v and c) FFR_A7v with d) a zoom of FFR_A7v's penetration (the grey area represents the average penetration (standard deviation) of FFR_A1, as reference).

Comparison of pressure drops, maximum penetrations and MPPS

Table 2 presents the pressure drop measurements (N=3) obtained at the beginning of the penetration experiments, as well as the average maximum penetration (N=3), and the MPPS at which it was obtained. One can note that FFRs from manufacturer C exhibit higher pressure drops compared to those from manufacturers A and B. However, all measured pressure drops remain well below the normative limit of 3.43 mbar.

Table II. Pressure drops, maximum penetrations and MPPS for the 12 FFRs used in this study.

Designation	Pressure drop (mbar)	Maximum penetration (%)	MPPS (nm)
FFR_A1	0.91 ± 0.07	2.84 ± 0.95	39.2
FFR_A1v	0.98 ± 0.12	3.85 ±0.86	39.2
FFR_B	0.83 ± 0.11	2.52 ± 0.35	45.3
FFR_Bv	1.00 ± 0.06	3.25 ± 0.09	45.3
FFR_C	1.35 ± 0.04	2.67 ± 0.63	52.3
FFR_Cv	1.09 ± 0.05	3.13 ± 2.06	52.3
FFR_A2	0.34 ± 0.01	2.20 ± 0.30	34
FFR_A3	0.70 ± 0.03	1.25 ± 0.53	29.4
FFR_A4v	1.67 ± 0.15	1.45 ± 0.07	39.2
FFR_A5	0.62 ± 0.57	0.52 ± 0.07	29.4
FFR_A6v	1.24 ± 0.02	0.30 ± 0.06	29.4
FFR_A7v	1.16 ± 0.04	0.02 ± 0.01	39.2

The presence of a valve does not alter the MPPS. However, when a valve is present. Both penetration and pressure drop increases slightly. This phenomenon is likely attributable to a reduction in the effective filtration surface area caused by the valve, which consequently elevates the face velocity across the FFR. This higher velocity leads to two consequences: it diminishes particle capture efficiency particularly for nano-sized particles (Abdolghader *et al.*, 2018) and impose a higher aerodynamic resistance, resulting in higher penetration and pressure drop through the FFR.

The values in Table II also show that the difference in FFR classification (N-, R-, or P-rated), although it affects maximum penetrations and pressure drops, has very little effect on the MPPS range and the trends in the penetration curves.

DISCUSSION

The benchmark conducted in this study confirms that penetration measurements for all tested FFRs comply with normative limits and demonstrates that the setup and methodology reliably deliver expected results. Although test conditions differ slightly from normative standards, the measurements align with expected values. Additionally, this study provides detailed penetration profiles by particle size, offering precise MPPS determination and insights beyond standard certification data.

Maximum penetration values remain below 5%, and the MPPS consistently falls under 100 nanometers, typically between 30 and 50 nanometers for electret media. These results indicate similar penetration trends across different models: penetration decreases for particles smaller or larger than the MPPS, approaching zero at the extremes.

Notably, FFRs from manufacturer C exhibit higher pressure drops and MPPS compared to those from manufacturers A and B. These findings align with previously reported data for FFR_A1, suggesting that initial penetration characteristics are comparable across models under standardized conditions.

However, this study did not address variables such as filtration airflow rate, breathing patterns, clogging effects, or relative humidity. Previous research indicates these factors can influence penetration, but such conclusions cannot be generalized without further testing. Future work should explore whether variations in operational conditions or extended use affect penetration similarly across different FFRs.

CONCLUSIONS

The test setup used for this study provides reliable measurements of penetration as a function of particle size and of pressure drop, confirming compliance with normative standards and revealing consistent MPPS behavior among FFRs. These results suggest that initial performance trends observed for FFR_A1 may be extrapolated to other models under similar conditions.

Nevertheless, broader applicability requires additional research on factors such as clogging, cyclic breathing, intensity of respiration, and exposure to liquid particles. Investigating these aspects will help determine whether current findings hold under real-world conditions.

ACKNOWLEDGMENTS

The authors would like to acknowledge the IRSST (Institut de recherche Robert Sauvé en Santé et en sécurité du Travail) for the financial support of this work.

REFERENCES

Abdolghader, P., C. Brochot, F. Haghighat, and A. Bahloul (2018). *Airborne nanoparticles filtration performance of fibrous media: A review*. Science and Technology for the Built Environment, 24: 648–672.

Andraos C, M. Gulumian, G. Ichihara, B. Kim and I. J. Yu (2022) *Editorial: Occupational exposure to nanomaterials*, Frontiers in Toxicology, 4:1014600.

Asadi S., Cappa C. D., Barreda S., Wexler A. S., Bouvier N. M. and Ristenpart W. D. (2020) *Efficacy of masks and face coverings in controlling outward aerosol particle emission from expiratory activities*, Scientific Reports, 10: 15665.

Bahloul A., Brochot C. and Layne B. (2021) *Leakage versus Material Filtration in Barrier Facemask Efficiency*, Health, 13: 439-53.

Bahloul A., Mahdavi A., Haghighat F. and Ostiguy C. (2014) *Evaluation of N95 filtering facepiece respirator efficiency with cyclic and constant flows*, Journal of Occupational and Environmental Hygiene, 11: 499-508.

Balazy A., Toivola M., Reponen T., Podgorski A., Zimmer A. and Grinshpun S. A. (2005) *Manikin-Based Performance Evaluation of N95 Filtering-Facepiece Respirators Challenged with Nanoparticles*, The Annals of Occupational Hygiene, 50: 259-69.

Bourrous S., Barrault M., Mocho V., Poirier S., Bardin-Monnier N., Charvet A., Thomas D., Bescond A., Fouqueau A., Mace T., Gaie-Levrel F. and Ouf F.-X. (2021) *A Performance Evaluation and Inter-laboratory Comparison of Community Face Coverings Media in the Context of COVID-19 Pandemic*, Aerosol and Air Quality Research, 21: 200615.

Brochot C., Djebara A. , Haguiguat F. and Bahloul A. (2015) *Validation of a Laboratory Test Bench for the*

Efficiency of an N95 Filtering Face Piece, using Simulated Occupational Exposure, Journal of Environmental and Analytical Toxicology, 5: 286.

Brochot C., Haghighat F. and Bahloul A. (2020a) *Comparative Performance of the NanoScan and the Classic SMPS in Determining N95 Filtering Facepiece Efficiency Against Nanoparticles*, Aerosol Science and Engineering, 4: 178-91.

Brochot C., M. N. Saidi, and A. Bahloul. (2020b) *Qualitative Knowledge of Filtering Facepiece Respirators for Filtration Performance Tests during the COVID-19 Pandemic*, Journal of the International Society for Respiratory Protection, 37: 94-107.

Brochot C., M. N. Saidi, and A. Bahloul. (2020c) *How Effective Is the Filtration of 'KN95' Filtering Facepiece Respirators During the COVID-19 Pandemic?*, Annals of Work Exposures and Health, 65: 358-66.

Canadian Standards Association (CSA) (2021) Canadian Standards Association Z94.4.1 : 21 Performance of filtering respirators In.: Ontario, Canada.

Code of Federal Regulations (CFR) (1995) 42 CFR, Part 84, Respiratory Protection Devices. In. Washington.

Corbin J. C., G. J. Smallwood, I. D. Leroux, J. N. Oliaee, F. Liu, T. A. Sipkens, R. G. Green, N. F. Murnaghan, T. Koukoulas and P. Lobo. (2021) *Systematic experimental comparison of particle filtration efficiency test methods for commercial respirators and face masks, Scientific Reports*, 11:1.

Chen, YH., D. Nguyen, S. Brindley, T. Ma, T. Xia, J. Brune J. M. Brown and C. S.-J. Tsai (2023) *The dependence of particle size on cell toxicity for modern mining dust*, Scientific Reports, 13.

Drewnick, F., J. Pikmann, F. Fachinger, L. Moormann, F. Sprang and S. Borrmann *Aerosol filtration efficiency of household materials for homemade face masks: Influence of material properties, particle size, particle electrical charge, face velocity, and leaks,* Aerosol Science and Technology, 55: 63–79.

Eninger R. M., Honda T., Reponen T., McKay R. and Grinshpun S. A. (2008) *What Does Respirator Certification Tell Us About Filtration of Ultrafine Particles?*, Journal of Occupational and Environmental Hygiene, 5: 286-95.

Essa, W.K., S. A. Yasin, I. A. Saeed, and G. A. M. Ali (2021) Nanofiber-Based Face Masks and Respirators as COVID-19 Protection: A Review, Membranes, 11: 250.

Freeman C., Burch R., Strawderman L., Black C., Saucier D., Rickert J., Wilson J., Seitz H. and Stull J. (2022) *Do They Really Work? Quantifying Fabric Mask Effectiveness to Improve Public Health Messaging*, International Journal of Environmental Research and Public Health, 19: 6372.

Hao W., Parasch A., Williams S., Li J., Ma H., Burken J. and Wang Y. (2020) *Filtration performances of non-medical materials as candidates for manufacturing facemasks and respirators*, International Journal of Hygiene and Environmental Health, 229: 113582.

Haruta H., Honda T., Eninger R. M., Reponen T., McKay R. and Grinshpun S. A. (2008) *Experimental and theoretical investigation of the performance of N95 respirator filters against ultrafine aerosol particles tester at constant and cyclic flows*, Journal of the International Society for Respiratory Protection, 25: 75-88.

Kim J., Park J., Tsai P.-J. and Yoon C. (2024) *The Effects of Temperature and Humidity on Electrostatic Changes in Respirators and Their Filtration Efficiency*, Indoor Air, 2024: 5503400.

Konda A., Prakash A., Moss G. A., Schmoldt M., Grant G. D. and Guha S. (2020) *Aerosol Filtration Efficiency of Common Fabrics Used in Respiratory Cloth Masks*, ACS Nano, 14: 6339-47.

Kumar A., Joshi S., Venkatesan S. and Balasubramanian V. (2022) *A detailed investigation of N95 respirator sterilization with dry heat, hydrogen peroxide, and ionizing radiation*, Journal of Industrial Textiles, 51: 378S-405S.

Mahdavi A., Bahloul A., Haghighat F. and Ostiguy C. (2014) *Contribution of breathing frequency and inhalation flow rate on performance of N95 filtering facepiece respirators*, The Annals of Occupational Hygiene, 58: 195-205.

Mahdavi A., Haghighat F., Bahloul A., Brochot C. and Ostiguy C. (2015) *Particle loading time and humidity effects on the efficiency of an N95 filtering facepiece respirator model under constant and inhalation cyclic flows*, The Annals of Occupational Hygiene, 59: 629-40.

Marchais G., Arbane M., Topilko B., Brousseau J., Brochot C., Yaddaden Y., Bahloul A. and Maldague X. (2025) *SafeRespirator: Comprehensive Database for N95 Filtering Facepiece Respirator Leakage*

Detection Including Infrared, RGB Videos, and Quantitative Fit Testing, IEEE Access, 13: 1-12.

McAvoy M., Bui A.-T. N., Hansen C., Plana D., Said J. T., Yu Z., Yang H., Freake J., Van C., Krikorian D., Cramer A., Smith L., Jiang L., Lee K. J., Li S. J., Beller B., Huggins K., Short M. P., Yu S. H., Mostaghimi A., Sorger P. K. and LeBoeuf N. R. (2021) *3D Printed frames to enable reuse and improve the fit of N95 and KN95 respirators*, BMC Biomedical Engineering, 3: 10.

National Institute for Occupational Safety and Health (NIOSH) (2015) Hierarchy of Controls. https://www.cdc.gov/niosh/topics/hierarchy/.

National Institute for Occupational Safety and Health (NIOSH) (2021) Current Intelligence Bulletin 70: health effects of occupational exposure to silver nanomaterials. Publication No. 2021-112, https://doi.org/10.26616/NIOSHPUB2021112.

Ng I., Kave B., Begg F., Bodas C. R., Segal R. and Williams D. (2022) *N95 respirators: quantitative fit test pass rates and usability and comfort assessment by health care workers*, Medical Journal of Australia, 217: 88-93.

O'Shaughnessy, P. T., B. Strzelecki, M. Ortiz-Hernandez P. Aubin, X. Jing, Q. Chang, J. Xiang, P.S. Thorne and J. T. Stapleton (2021) *Characterization of performance and disinfection resilience of nonwoven filter materials for use in 3D-printed N95 respirators,* Journal of Occupational and Environmental Hygiene, 18: 265–275.

O'Shaughnessy P. (2022) *Review and demonstration of equations applied to models of filtering facepiece respirator particle capture efficiency*, Journal of Occupational and Environmental Hygiene, 19: 615-628.

Peters A., Palomo R., Ney H., Lotfinejad N., Zingg W., Parneix P. and Pittet D. (2021) *The COVID-19 pandemic and N95 masks: reusability and decontamination methods*, Antimicrobial Resistance & Infection Control, 10: 83.

Richardson A. W., Eshbaugh J. P. and Hofrace K. C. (2006) *Respirator filter efficiency testing against particulate and biological aerosols under moderate to high flow rates,* In.: Edgewood Chemical Biological Center.

Rengasamy, S., A. Miller and B. C. Eimer (2011). *Evaluation of the Filtration Performance of NIOSH-Approved N95 Filtering Facepiece Respirators by Photometric and Number-Based Test Methods*. Journal of Occupational and Environmental Hygiene, 8: 23–30.

Schraufnagel, D.E. (2020) *The health effects of ultrafine particles*. Experimental and Molecular Medicine, 52.

Sharma A., Omidvarborna H. and Kumar P. (2022) *Efficacy of facemasks in mitigating respiratory exposure to submicron aerosols*, Journal of Hazardous Materials, 422: 126783.

Sharma S., Wang F., Kumar S., Nawal R. R., Kumar P., Yadav S., Szenti I., Kukovecz A., Schiller U. D. and Rawal A. (2022) *Structural and functional integrity of decontaminated N95 respirators: Experimental results*, Journal of Industrial Textiles, 51: 7999S-8017S.

Turgeon N., Pagé M., Robillard J., Goulet V., Bahloul A., Brochot C., Saidi M. N., Dumont-Leblond N. and Duchaine C. (2023) *Filtration performance, fit test and side effects of respiratory personal protective equipment following decontamination: Observations for user safety and comfort*, PLoS One, 18: e0280426.

Yang W., Myers W. R., Bergman M., Fisher E., Ryan K. J., Vollmer B., Portnoff L. and Zhuang Z. (2025a) *Total outward leakage of face-worn products used by the general public for source control*, American Journal of Infection Control, 53: 239-44.

Yang W., Myers W. R., Bergman M., Fisher E., Ryan K. J., Vollmer B., Portnoff L. and Zhuang Z. (2025b) *Evaluating source control efficacy against exhaled submicron particles: Total outward leakage of surgical masks and half facepiece respirators across a spectrum of particle sizes*, Aerosol Science and Technology, 59: 487-98.

Zangmeister C. D. , J. G. Radney, E. P. Vicenzi, and J. L. Weaver (2020) *Efficiencies of Nanoscale Aerosol by Cloth Mask Materials Used to Slow the Spread of SARS-CoV-2*, ACS Nano, 14: 9188-9200.

Zhu J., Jiang Q., He X., Li X., Wang L., Zheng L., Jing P. and Chen M. (2022) *Filtration efficiency of N95 filtering facepiece respirators during multi-cycles of '8-hour simulated donning + disinfection'*, Journal of Hospital Infection, 127: 91-100.